DOI https: //doi. org/10.1007/s11595-020-2241-5

# Effect of Zn/Mg/Cu Additions on Hot Cracking Tendency and Performances of Al-Cu-Mg-Zn Alloys for Liquid Forging

**SUN Yonggen[1], DU Zhiming[1*], SU Yanni[2], CHENG Yuansheng[2], LIU Yongwang[2]**

*(1. National Key Laboratory for Precision Hot Processing of Metals, Harbin Institute of Technology, Harbin 150001, China; 2. School of Materials Science and Engineering, Harbin Institute of Technology, Harbin 150001, China)*

**Abstract:** During the process of liquid forging, a host of hot cracking defects were found in the Al-Cu-Mg-Zn aluminum alloy. Therefore, mechanical tests and analyses by optical microscope, scanning electron microscope, and X-ray diffraction were performed to research the influences of zinc, magnesium, and copper (three main alloying elements) on hot cracking tendency and mechanical properties. It was concluded that all the three alloying elements exerted different effects on the performances of newly designed alloys. And the impact of microstructures on properties of alloys was stronger than that of solution strengthening. Among new alloys, Al-5Cu-4.5Mg-2.5Zn alloy shows better properties as follows: $\sigma b$=327 MPa, $\delta$=2.7%, HB=107 N/mm$^2$, and HCS=40.

**Key words:** liquid forging; Al-Cu-Mg-Zn alloys; mechanical properties; hot cracking tendency

# 1 Introduction

Aluminum alloys have been extensively used in industrial productions instead of steel structures, such as aircraft structural parts, tank track plates and automotive pistons[1-3]. With increasing lightweight requirements, high-strength aluminum alloys have been widely studied and applied[4-7]. However, traditional die forging technology can not completely meet manufacturing and performance requirements, which makes the study of liquid forging technology widely concerned[8,9].

Liquid forging is a process that certain amount of molten metal is poured directly and filled the dies, solidified and crystallized with plastic deformation under applied pressure, to obtain knitted net-shape parts[10]. It is a metal forming technology which could save time, energy and materials[11]. And the technology shows great prospects considering the properties and the technology processes[12].

However, liquid forging technology is primarily dominated by solidification, so it is demanding to avoid hot cracks that caused by uneven stresses. The problem seriously restricts the development of liquid forging forming technology[10].

In this paper, these fundamental problems of aluminum alloys for liquid forging technology were discussed. How to solve the defects of hot cracks during liquid forging was researched in term of alloying elements. And the influences of zinc, magnesium, and copper on hot cracking tendency and microstructures of Al-Zn-Mg-Cu alloys were analyzed, so that it could provide a theoretical basis for fabrication of high-strength alloys with a low hot cracking tendency and excellent performances.

# 2 Experimental

## 2.1 Component design and alloy melting

Chemical components of 2024 alloy were shown in Table 1. Alloying components were designed by single variable methods based on the 2024 alloy. The new kinds of aluminum alloys were prepared by adding industrial pure zinc, industrial pure magnesium and Al-Cu (50%) intermediate alloy.

In order to weaken hot cracking tendency and satisfy the strength, hardness and toughness demands, it was indispensable to ensure that the content of zinc was less than 6%, and that the one of magnesium was higher than 2% and that the copper content was higher than 1.5%[14]. The composition ratio of main alloying elements was optimized by considering theoretical lim-

---



(Received: Jan. 29, 2019; Accepted: Oct. 16, 2019)

SUN Yonggen (孙永根) : Ph D; E-mail: hitsunyg@163.com;

*Corresponding author: DU Zhiming (杜之明) : Prof.; Ph. D; E-mail: duzm@263.net

Funded by the International Cooperation Project of the Ministry of Science and Technology of China (No. 2014DFR50320) and the National Natural Science Foundation of China (No. 51174064)

it contents and $1_{st}$-$11_{th}$ alloys were designed as shown in Table 2.

**Table 1 Chemical components of 2024 alloy**

| Elements/wt% | Cu | Mg | Zn | Cr | Mn | Ti | Fe | Si | Al |
|---|---|---|---|---|---|---|---|---|---|
| 2024 | 4.90 | 1.13 | 0.10 | 0.01 | 0.82 | 0.04 | 0.20 | 0.20 | others |

**Table 2 Component proportions of designed alloys**

| Number | Mass fractions /wt% | | |
|---|---|---|---|
| | Zn | Mg | Cu |
| 1 | 2.1-3.0 | 3.0-3.9 | 4.5-5.4 |
| 2 | 3.1-4.0 | | |
| 3 | 4.1-5.0 | | |
| 4 | 5.1-6.0 | | |
| 5 | 2.1-3.0 | 1.0-1.9 | 4.5-5.4 |
| 6 | | 2.0-2.9 | |
| 7 | | 4.0-4.9 | |
| 8 | 2.1-3.0 | 3.0-3.9 | 1.5-2.4 |
| 9 | | | 2.5-3.4 |
| 10 | | | 3.5-4.4 |
| 11 | | | 5.5-6.4 |

The additions were weighed according to the design as showed in Table 2. With melting furnace heated to 350 ℃, 2024 alloy and Al-Cu (50%) intermediate alloy were added and heated up to 750 ℃, stirred until melted. Then a bit of NaCl & KCl covering agent was sprinkled. The furnace was cooled to 700 ℃, pure magnesium and pure zinc was added respectively and dissolved. When furnace temperature was heated back to 750 ℃, the melted alloy was refined twice by $C_2Cl_6$.

### 2.2 Liquid forging forming

Liquid forging dies were assembled and preheated to 300 ℃, whose surfaces were sprayed with graphite. The melt heated to 730 ℃ was poured into the set of cylindrical dies, applied quickly with pressure holding 30 seconds by forging hydraulic machine. The cylinder parts were prepared, which were 65 mm in diameter and 60 mm in height.

### 2.3 Hot cracking tendency and mechanical property

The constrained rod casting showed in Fig.1 was used to evaluate the hot cracking tendency of newly designed alloys. Specimens were observed and hot cracking susceptibility (*HCS*) indexes were calculated by Formula 1, characterized as hot cracking tendency.

$$HCS=\sum(\omega_{crack}\cdot f_{length}\cdot f_{location}) \quad (1)$$

where *HCS* is short for hot cracking susceptibility; $f_{length}$ is rod length factor, as showed in Fig.2(a), which indicates the difficulty level of hot cracking; $f_{location}$ is crack location factor (Fig.2(b)); $\omega_{crack}$ is crack size factor, where the rod with or without cracks, semi-hairline, hairline, semi-broken and fracture five levels, corresponding $\omega_{crack}$ values 0-4[14], respectively.

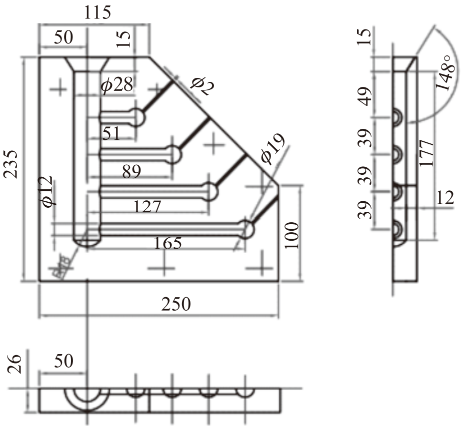


Fig.1 Constrained rod casting (*CRC*) mold (Unit: mm)[13]

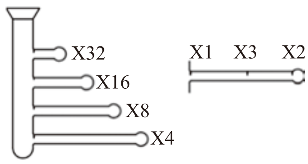


Fig.2 Determining crack sensitivity from widths of cracks in *CRC*[14]: (a) Rod length factors; (b) Crack location factors

Tensile strength and elongation of new alloys were measured by the electronic universal testing machine (INSTRON-5569, Boston, USA) at room temperature (25 ℃). The tensile rate was 1.0 mm/min. And the hardness was tested by Brinell hardness tester (HB-3000B, Shandong, China). The load was 2 452 N and holding time was the 30 s. X-ray diffraction (XRD, D/MAX-RB, Rigaku, Japan) was used for phase analysis of different aluminum alloys. After coarse grinded, fine grinded, polished, and etched, microstructures were observed on the metallographic microscope (*MM*, OLYMPUS-PEM-3, Hatagaya, Japan), and phase distributions were observed by scanning electron microscope (SEM, SUPRA-55, Oberkochen, Germany).

## 3 Results and discussion

### 3.1 Analysis of heat cracking and microstructure

The microstructures of new alloy formed by liquid forging were mixed organizations consisting of free dendrites and equiaxed grains, as showed in Fig.3. Meanwhile, there were numerous net-like and non-equilibrium eutectic structures distributed along grain boundaries. During the liquid forging process, there was a different temperature distribution in alloy melt. The outer melt was rapidly nucleated and grew, formed fine equiaxed grains because of numerous nucleation particles. The internal nucleation particles were a bit. And the crystallizing latent heat made crystal nucleus grow up rapidly and form dendrites. Under applied loads, dendrites were deformed and broken into rose-shape organizations. Solidification was simultaneously too fast, and alloy elements distributed unevenly. So microstructures deviated from equilibrium state in different levels.

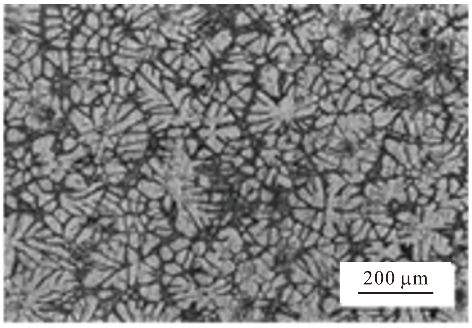


Fig.3 The microstructures of designed aluminum alloy

In general, the properties of most new alloys were better than that of 2024 alloy as Fig.4. Tensile strength was about 220-320 MPa. The elongation performed poorly, which mostly reached about 2%. While the copper was lower, the elongations of 8th and 9th alloys were more than 15%. And the Brinell hardness was about 100 N/mm$^2$, excepting that of the 8th and 9th alloys were evidently lower (58.4 and 86.8 N/mm$^2$, respectively).

## 3.2 Effect of zinc content on microstructure and properties of new alloys

When other element contents were constant, under the condition that zinc content was less than 6%, as showed in Fig.5, the hot cracking tendency of new alloys dropped with the decrease of zinc content. However, as zinc content was less than 3%, the hot cracking properties had no fluctuation with zinc content changing. Meanwhile, with increasing zinc content, the strength showed a little change, which was about 290 MPa. But the elongation degraded. If the zinc content was about 2%-3%, the elongation reached the maximum, 3.3%. The hardness improved with the increase of zinc content, but the variation was also less, and the Brinell hardness was maintained about 100-115 N/mm$^2$. Consequently, zinc content in new alloys should be kept at a relatively low level, while the strength and elongation were larger, which was 308 MPa and 3.3%, respectively, and the Brinell hardness was 104 N/mm$^2$.

The new alloys were composed of phases *S* ($Al_2CuMg$), phases $\theta$ ($Al_2Cu$), phases $\eta$ ($MgZn_2$), and aluminum matrix (Fig.6). Zinc basically had no effect on phases formation of new alloys. Microstructures of 1st-4th alloys in Fig.7 showed zinc element was basically dissolved in aluminium. And phases *S* and phases $\theta$ were concentrated along the boundaries, while small amounts of phases dispersed in grains.

1st is Al-5Cu-3.5Mg-2.5Zn alloy; 2nd is Al-5Cu-3.5Mg-3.5Zn alloy; 3rd is Al-5Cu-3.5Mg-4.5Zn alloy; 4th is Al-5Cu-3.5Mg-5.5Zn alloy.Zinc element had a greater solubility in aluminum (the ultimate was about 70.0%[15]) and it was mainly functioned as solution strengthening element. Zinc element was mostly dissolved in the aluminum matrix to form solid solutions. The strength and hardness were improved with the increase of zinc content. The zinc uniformly distributed in the matrix, causing hardness enhancement of

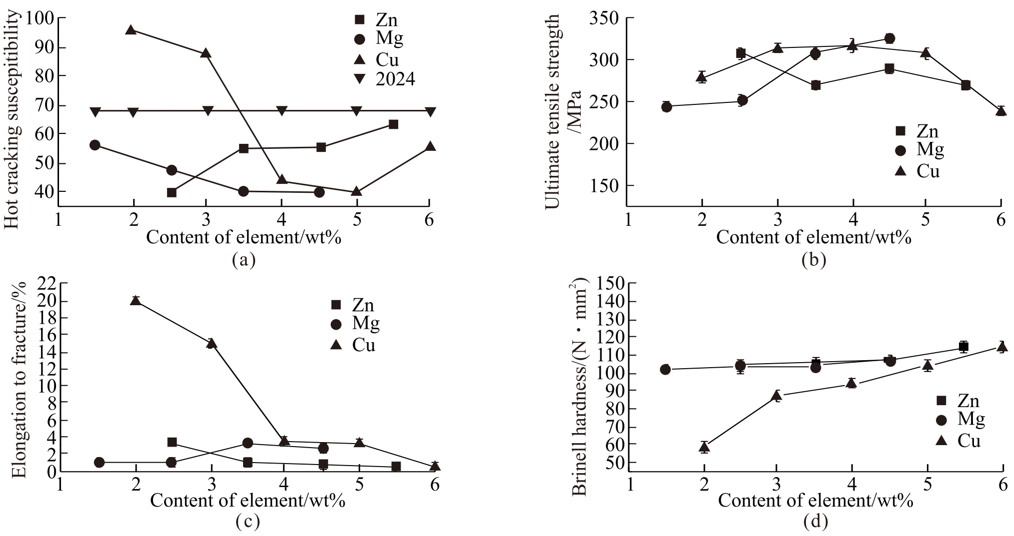


Fig.4 Influence of zinc, magnesium and copper contents on properties of aluminum alloys: (a) Hot cracking tendency; (b) Tensile strength; (c) Elongation; (d) Brinell hardness (Note: the samples' number of each alloy is 5)

the new alloys. With gradually adding zinc, solute concentrations of solid solutions $\alpha$ (Al) were increased. However, copper and magnesium in alloy crystal were segregated to form more eutectic structures distributed in the boundaries, causing strength and hot cracking tendency worse.

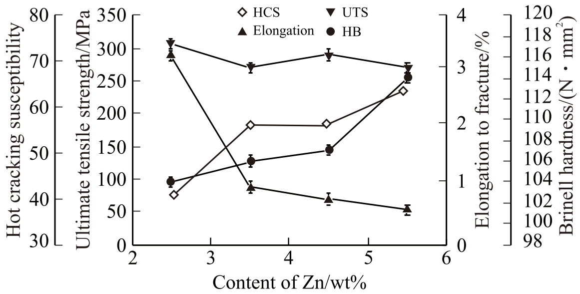


Fig.5 Influence of zinc on properties of aluminum alloys (Al-5Cu-3.5Mg-*x*Zn) (Note: the samples' number of each alloy is 5)

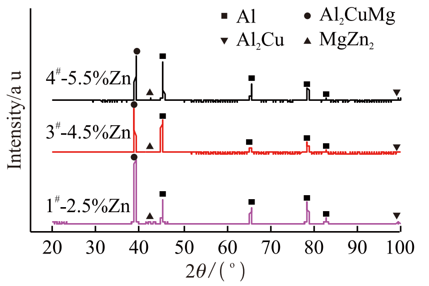


Fig.6 X-ray diffraction results of 1st, 3rd and 4th alloys (Al-5Cu-3.5Mg-*x*Zn)

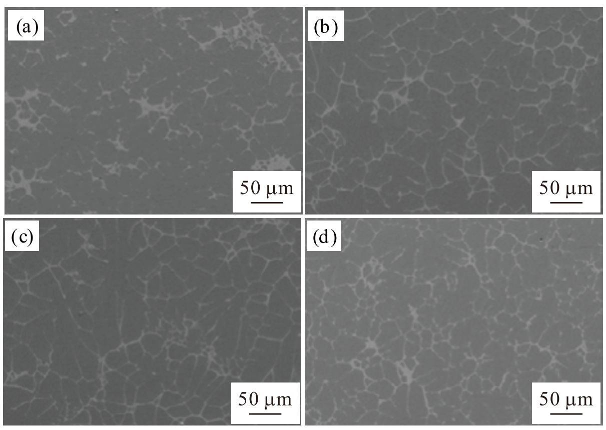


Fig.7 Scanning electron micrographs of new alloys with different zinc contents: (a) 1st alloy; (b) 2nd alloy; (c) 3rd alloy; (d) 4th alloy

It was found that eutectic structures along grain boundaries exerted a weakening effect on tensile strength. Moreover, the more continuous distribution of second phases were, the lower was the strength. But the hot cracking property was better.

The eutectic microstructure of 1st alloy (Al-5Cu-3.5Mg-2.5Zn) as showed in Fig.7 was coarse and dispersed, obviously different from others. The microstructures of the 2nd, 3rd, and 4th alloys had little diverseness, and the strength were basically parallel. According calculation, the eutectic microstructure of 1st alloy accounted for the lowest percentage (about 7%), and tensile strength was the highest, reaching at 308 MPa, and the hot cracking tendency was the lowest (*HCS* was about 40).

### 3.3 Effect of magnesium on microstructure and properties of new alloys

As showed in Fig.8, when magnesium content was about 3%-5%, the hot cracking tendency was minimized (*HCS* was only 40). Nevertheless, the *HCS* increased following the content lessened when it dropped to less than 3%. When the content varied from 1% to 5%, the strength and hardness increased gradually. And as it was about 4%-5%, the strength reached at 327 MPa, which was the highest, while the maximum hardness was 107 N/mm$^2$. The elongation increased firstly and then decreased. When the content kept at a level of about 3%-4%, the elongation also reached at a maximum of 3.3%.

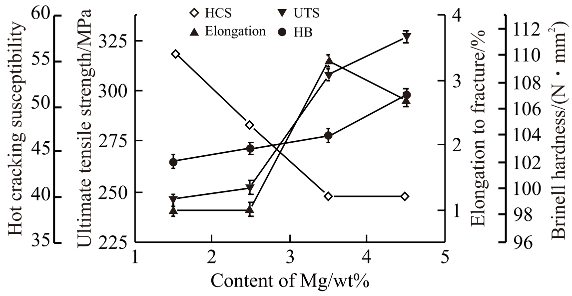


Fig.8 Influence of magnesium on properties of aluminum alloys (Al-5Cu-*x*Mg-2.5Zn) (Note: the samples' number of each alloy is 5)

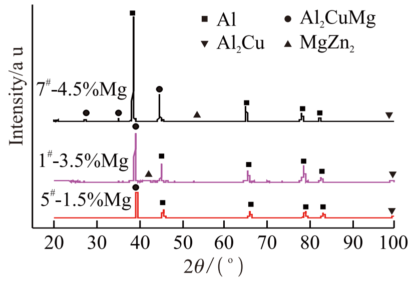


Fig.9 X-ray diffraction results of 5th, 1st and 7th alloys (Al-5Cu-xMg-2.5Zn)

The XRD analysis results of 7th, 1st, 5th alloys in Fig.9 (magnesium decreasing trend) showed Mg content could change the phase compositions. When magnesium declined, the amount of phases $\eta$ ($MgZn_2$) descended or even disappeared, which made its dispersion and strengthening effects weakened, so the strength and hardness were minimized. The ultimate solubility of magnesium was 17.4% in aluminum [15]. Magnesium contents of 5th, 6th, 1st, and 7th alloys varied from 1% to 5%, and parts of magnesium were dissolved in solid solution α (Al). At this moment, solidification strengthening was dominant, and the strength and hardness rose with increasing magnesium. The other parts of magnesium formed eutectic structures with copper along grain boundaries. The effect was weakened when magnesium content reduced and the hot cracking tendency would fortify. Meanwhile, eutectic structures distributing in matrix affected properties of alloys, especially the elongation.

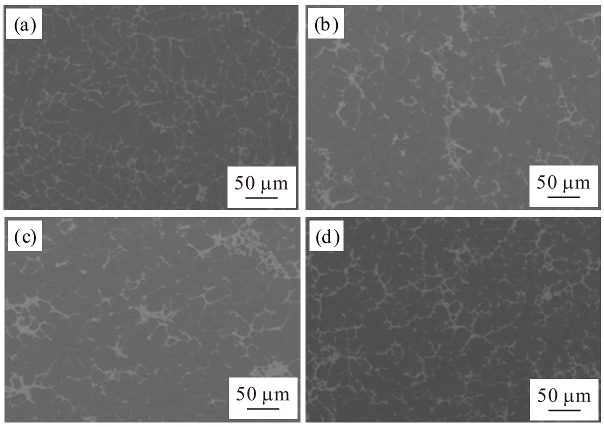


Fig.10 Microstructures of alloys with different magnesium contents: (a) 5th alloy; (b) 6th alloy; (c) 1st alloy; (d) 7th alloy

In 7th alloy (Al-5Cu-4.5Mg-2.5Zn) (Fig.10), the magnesium content was highest and the percentage of eutectic structures containing phases *S* ($Al_2CuMg$) and phases $\theta$ ($Al_2Cu$) was the lowest, which was only 6.2%, and the strength was the highest at this point (about 327 MPa). Compared with 5th alloy, whose eutectic percentage was about 6.5%, the distribution of eutectic structures of the 7th alloy was more discrete and the diffusely distributed second phases were more. So it was visible that a growing number of eutectic structures made the impact of solid solution strengthening weakened, even making mechanical properties sharply reduced[16]. The percentage of eutectic microstructures in the 1st alloy (Al-5Cu-3.5Mg-2.5Zn) was 7%, but these phases were diffusely distributed in the alloy, therefore mechanical properties of the 1st alloy were also well.

5th is Al-5Cu-1.5Mg-2.5Zn alloy; 6th is Al-5Cu-2.5Mg-2.5Zn alloy; 1st is Al-5Cu-3.5Mg-2.5Zn alloy; 7th is Al-5Cu-4.5Mg-2.5Zn alloy.

### 3.4 Effect of copper content on microstructure and properties of new alloys

When the condition that other element contents were constant, and that copper content was less than 6% and higher than 4%, the hot cracking properties dwindled along with decreasing copper content in Fig.11. But when copper content was less than 4%, with the decrease of copper content, the hot cracking tendency increased sharply, which was as high as 88 or 96. The strength improved with the increase of copper content, and when copper content was higher than 5%, the strength dropped drastically. The effect of copper content on elongation was also large. When the content of copper was less than 4%, the elongation decreased sharply following the increase of copper content. But when it was higher than 4%, the elongation kept only 1%. The hardness increased with increasing copper, and the highest Brinell hardness was 114 N/mm$^2$.

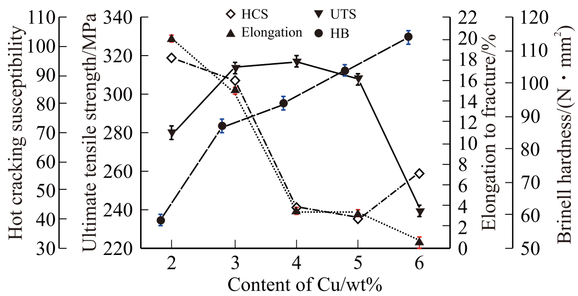


Fig.11 Influence of copper on the properties of aluminum alloys (Al-*x*Cu-3.5Mg-2.5Zn) (Note: the samples' number of each alloy is 5)

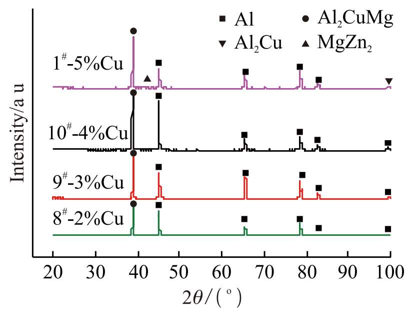


Fig.12 X-ray diffraction results of 1st, 10th, 9th and 8th alloys (Al-*x*Cu-3.5Mg-2.5Zn)

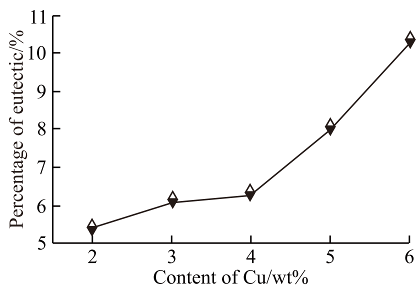


Fig.13 Effect of copper content on the percentage of eutectic structures in alloys

XRD analysis results of 1st, 10th, 9th and 8th alloys in Fig.12 showed phases $\theta$ ($Al_2Cu$) disappeared as copper content decreased. The solubility of copper in aluminum was very small (only 5.7%), so the copper element could not be dissolved in solid solution[15].

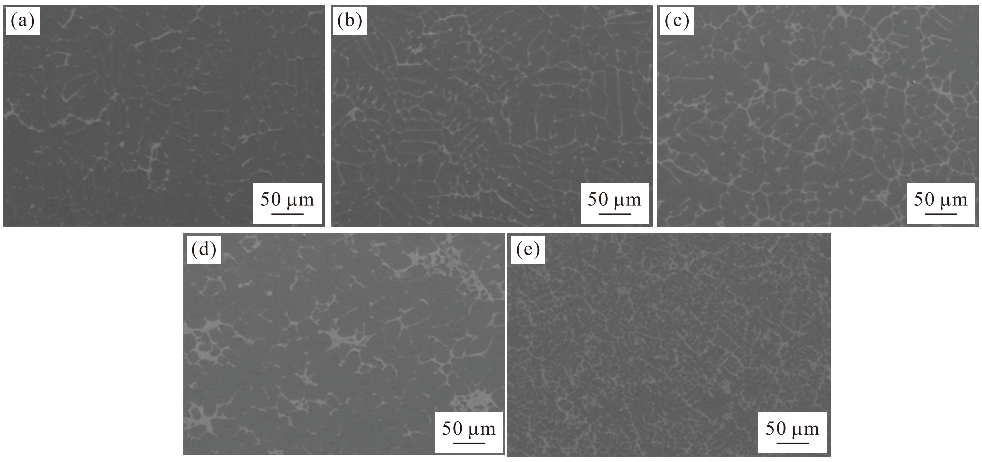


Fig.14 Microstructures of alloys with different copper contents: (a) 8th alloy; (b) 9th alloy; (c) 10th alloy; (d) 1st alloy; (e) 11th alloy (8th is Al-2Cu-3.5Mg-2.5Zn alloy; 9th is Al-2Cu-3.5Mg-2.5Zn alloy; 1st is Al-5Cu-3.5Mg-2.5Zn alloy; 11th is Al-5Cu-3.5Mg-2.5Zn alloy)

With augmented copper content, solid solution $\alpha$ (Al) had no change, and solid solution strengthening remained. Copper was continuously discharged into the aluminum liquid during solidification process, and solute concentration of liquid phase was continuously increased, then it could quickly meet the necessary conditions for eutectic reaction, to form net-like eutectic organizations along grain boundaries. By statistical analysis, when the copper content was 2%, the percentage of eutectic organizations was 5.3%, and when the copper content was increased to 6%, the percentage reached at 10.5% (Fig.13).

The microstructures of 8th, 9th, 10th, 1st, 11th alloys were showed in Fig.14. With the increase of copper content, eutectic structures increased significantly, which played a dominant role in the destruction of new alloys' strength. The strength should be reduced theoretically. From experimental results, the strength increased firstly then decreased sharply. It was caused by the phase components. There were eutectic structures of phases $S$ ($Al_2CuMg$) and phases $\theta$ ($Al_2Cu$) formed by copper, magnesium and aluminum elements and single distribution of phases $\theta$ in the crystals, which simultaneously benefited from both solid solution and dispersion strengthening[17]. Moreover, the distribution of net-like eutectic structures tended to be discrete. So when the copper content was higher, the strength and hardness showed better. With copper content increasing, eutectic structures increased. Then the hot cracking tendency decreased. The toughness and plasticity of alloys were greatly damaged, and the elongation was drastically reduced. When the copper content was more than 5%, the dispersed phases $\theta$ were excess in the 11th alloy (Al-6Cu-3.5Mg-2.5Zn), showed in Fig.14(i) and 14(j). Phases $\theta$ could not be completely dissolved in solid solution $\alpha$ (Al), causing the continuity of alloy matrix to be seriously destroyed[18]. Then the strength and elongation of alloys were in a sharp decrease, and the hot crack tended to augment.

# 4 Conclusions

a) The structures of new alloy fabricated by liquid forging were a mixture of free dendrites and near-equiaxed grains, and net-like eutectic structures were distributed along grain boundaries.

b) The effect of zinc element was mainly determined by solid solution strengthening. When zinc content increased, the effect was enhanced, and the hardness was increased.

c) As magnesium content increased, the strength and hardness were increased. When magnesium content decreased, the hot cracking tendency of alloy increased.

d) The effect of copper was mainly determined by the eutectic structures and the dispersed second phases.

e) The effect of zinc, magnesium, and copper on properties of newly alloys was the most significant, and the effect of structures on properties of alloys was stronger than that of solid solution strengthening.

## References

[1] Kasilingam S, Iqbal M A, Chandel P S, *et al*. Study of the Constitutive Behavior of 7075-T651 Aluminum Alloy[J]. *International Journal of Impact Engineering*, 2017, 108: 171-190

[2] Coloma P S, Izagirre U, Belaustegi Y, *et al*. Chromium-Free Conversion Coatings Based on Inorganic Salts (Zr/Ti/Mn/Mo) for Aluminum Alloys Used in Aircraft Applications[J]. *Applied Surface Science*, 2015, 345: 24-35

[3] Park D H, Choi S W, Kim J H, *et al*. Cryogenic Mechanical Behavior

of 5 000- and 6 000-Series Aluminum Alloys: Issues on Application to Offshore Plants[J]. *Cryogenics*, 2015, 68: 44-58

[4] Xu Y Q, Tong C Y, Zhan L H, *et al*. A Low-Density Pulse-Current-Assisted Age Forming Process for High-Strength Aluminum Alloy Components[J]. *The International Journal of Advanced Manufacturing Technology*, 2018, 97(9-12): 3 371-3 384

[5] Cao J, Li F, Ma X, *et al*. Study of Fracture Behavior for Anisotropic 7050-T7451 High-Strength Aluminum Alloy Plate[J]. *International Journal of Mechanical Sciences*, 2017, 128-129: 445-458

[6] Alireza V, Santu R, Sunil G, *et al*. New Bayesian-Optimization-Based Design of High-Strength 7xxx-Series Alloys from Recycled Aluminum[J] *JOM*, 2018, 70(11): 2 704-2 709

[7] Benedetti M, Fontanari V, Bandini M, *et al*. High- and Very High-Cycle Plain Fatigue Resistance of Shot Peened High-Strength Aluminum Alloys: The Role of Surface Morphology[J]. *International Journal of Fatigue*, 2015, 70: 451-462

[8] Hawryluk M. Review of Selected Methods of Increasing the Life of Forging Tools in Hot Die Forging Processes[J]. *Archives of Civil and Mechanical Engineering*, 2016, 16(4): 845-866

[9] Xu W, Li W, Wang Y. Experimental and Theoretical Analysis of Wear Mechanism in Hot-Forging Die and Optimal Design of Die Geometry[J]. *Wear*, 2014, 318(1-2): 78-88

[10] Luo Sh J, Chen B G, Qi P X. *Liquid Die Forging and Squeeze Casting Technology*[M]. Beijing: Chemical Industry Press, 2007

[11] Xu H, Zhang X, Liu Y P. Mechanical Property and Corrosion Behavior of $SiC_p$/2A50 Composites Prepared by Liquid Forging[J]. *Rare Metal Materials and Engineering*, 2015, 44(6): 1 307-1 313

[12] Murali S. Liquid Forging of Thin Al-Si Structures[J]. *Journal of Materials Processing Technology*, 2010, 210(10): 1 276-1 281

[13] Kamga H K, Larouche D. Hot Tearing of Aluminium-Copper B206 Alloys with Iron and Silicon Additions[J]. *Materials Science and Engineering: A*, 2010, 527(27-28): 7 413-7 423

[14] Cao G, Kou S. Hot Cracking of Binary Mg-Al Alloy Castings[J]. *Materials Science and Engineering: A*, 2006, 417 (1-2): 230-238

[15] Wang Z J, Huang Y H, Yang Y, *et al*. Atomic-Size Effect and Solid Solubility of Multicomponent Alloys[J]. *Scripta Materialia*, 2015, 94: 28-31

[16] Tebib M, Samuel A M, Ajersch F, *et al*. Effect of P and Sr Additions on the Microstructure of Hypereutectic Al-15Si-14Mg-4Cu Alloy[J]. *Materials Characterization*, 2014, 89: 112-123

[17] Morelock C R, Gallington L C, Wilkinson A P. Solid Solubility, Phase Transitions, Thermal Expansion, and Compressibility in $Sc_{1-x}Al_xF_3$[J]. *Journal of Solid State Chemistry*, 2015, 222: 96-102

[18] Vintila R, Milligan J, Drew R A L, *et al*. Formation of Nanostructures and Solid Solubility Extension in Cryomilled Al-Cu and Al-Si Powders[J]. *Canadian Metallurgical Quarterly*, 2009, 48(1):33-44